Transgenic mice express human MPO −463G/A alleles at atherosclerotic lesions, developing hyperlipidemia and obesity in −463G males

Lawrence W. Castellani,* James J. Chang,† Xuping Wang,* Aldons J. Lusis,* and Wanda F. Reynolds[1,†]

Departments of Medicine, Microbiology, and Molecular Genetics,* University of California-Los Angeles, Los Angeles, CA 90095; and Sidney Kimmel Cancer Center,† San Diego, CA 92121

Abstract **Myeloperoxidase (MPO) is an oxidant-generating enzyme present in macrophages at atherosclerotic lesions and implicated in coronary artery disease (CAD). Although mouse models are important for investigating the role of MPO in atherosclerosis, neither mouse MPO nor its oxidation products are detected in lesions in murine models. To circumvent this problem, we generated transgenic mice expressing two functionally different human MPO alleles, with either G or A at position −463, and crossed these to the LDL receptor-deficient (LDLR$^{-/-}$) mouse. The −463G allele is linked to higher MPO expression and increased CAD incidence in humans. Both MPO alleles were expressed in a subset of lesions in high-fat-fed LDLR$^{-/-}$ mice, notably at necrotic lesions with cholesterol clefts. MPOG-expressing LDLR$^{-/-}$ males (but not females) developed significantly higher serum cholesterol, triglycerides, and glucose, all correlating with increased weight gain/obesity, implicating MPO in lipid homeostasis. The MPOG- and MPOA-expressing LDLR$^{-/-}$ males also exhibited significantly larger aortic lesions than control LDLR$^{-/-}$ males. The human MPO transgenic model will facilitate studies of MPO involvement in atherosclerosis and lipid homeostasis.—**Castellani, L. W., J. J. Chang, X. Wang, A. J. Lusis, and W. F. Reynolds. **Transgenic mice express human MPO −463G/A alleles at athrosclerotic lesions, developing hyperlipidemia and obesity in −463G males. *J. Lipid Res.* 2006.** 47: **1366–1377.**

Supplementary key words myeloperoxidase • atherosclerosis • hyperlipidemia • cholesterol • triglycerides • macrophage

Atherosclerosis is a chronic inflammatory disease in which macrophages accumulate in the vascular wall. The macrophages release oxidizing enzymes, including myeloperoxidase (MPO), which oxidizes LDL particles, producing a more atherogenic form that is taken up more effectively by macrophages to create foam cells (1).

Mounting evidence implicates MPO in atherosclerosis. MPO catalyzes a reaction between chloride and hydrogen peroxide to generate hypochlorous acid, whereas it reacts with nitrite and nitric oxide to produce reactive nitrogen intermediates (2). MPO and its oxidant by-products are present in atherosclerotic lesions, colocalizing with foam cell macrophages (3, 4), and are especially abundant at sites of thrombosis (5). MPO preferentially oxidizes apolipoprotein A-I (apoA-I), the major protein component of HDL, impairing ABCA1-mediated cholesterol efflux from cells (6, 7). Circulating MPO levels are higher in patients with coronary artery disease (CAD) (8, 9), whereas individuals with inherited MPO deficiencies have less cardiovascular disease (10). An MPO promoter polymorphism, −463 G/A, which alters expression levels (11, 12), has been associated with an increased incidence of CAD (13–15) and severity of atherosclerosis (16, 17). The −463G allele has been linked with higher MPO mRNA and protein expression than the −463A allele in human and transgenic mouse monocyte-macrophages (12).

Mouse models are important for investigations of the molecular pathways underlying atherosclerosis. To that end, an MPO knockout mouse was generated, but it unexpectedly developed larger lesions in the LDL receptor-deficient (LDLR$^{-/-}$) model (18, 19). Moreover, neither mouse MPO nor its specific product, 3-chlorotyrosine, was detected at lesions in LDLR$^{-/-}$ mice. Because of the lack of mouse MPO gene expression at lesions, the LDLR$^{-/-}$ mouse model cannot be used for analysis of MPO effects at these sites. However, in transgenic mice expressing human MPO, the enzyme is detected in lesions in the LDLR$^{-/-}$ model (12, 19) and has been correlated with increased lesion size (19).

The differential expression of mouse and human MPO genes may be attributable in part to the −463G/A polymorphism in an upstream Alu element containing nuclear

Manuscript received 6 January 2006 and in revised form 15 February 2006 and in re-revised form 16 March 2006 and in re-re-revised form 25 April 2006.

Published, JLR Papers in Press, April 25, 2006.
DOI 10.1194/jlr.M600005-JLR200

[1] To whom correspondence should be addressed.
e-mail: wreynolds@skcc.org

receptor response elements (11, 12). −463G enhances binding by the SP1 transcription factor (11), whereas −463A promotes binding by estrogen receptor α (ERα) (12, 20). An overlapping site is recognized by peroxisome proliferator-activated receptor γ (PPARγ) (12), a transcription factor that is expressed in foam cell macrophages at atherosclerotic lesions and regulates genes involved in inflammatory responses, including CD36 scavenger receptor (21), liver X receptor (22), and MPO (12). PPARγ ligands markedly upregulate MPO expression (~20-fold) in macrophage colony stimulating factor (MCSF)-treated cells (12). Estrogen blocks the effects of PPARγ, suggesting that ER binding sterically interferes with access by PPARγ. The −463A site is bound more effectively by ER, and estrogen blocks PPARγ induction more effectively. Thus, competition between PPARγ and ER may explain the lower expression of the MPO −463A allele, especially in females. Because Alu elements are primate-specific, the mouse MPO gene lacks this PPARγ binding site and is not upregulated by PPARγ ligands (12). This lack of PPARγ responsiveness may explain the absence of mouse MPO at atherosclerotic lesions in the LDLR$^{-/-}$ model.

To facilitate the investigation of MPO in atherosclerosis and other inflammatory diseases, we generated transgenic mice expressing the human MPO −463G or −463A allele under the control of native human promoter elements. The complex regulation by PPARγ, including the block by estrogen, is replicated in transgenic MPOG and MPOA mice (12). In LDLR$^{-/-}$ mice on an atherogenic diet, the human MPO −463G transgene was found to be expressed in aortic lesions, colocalizing with PPARγ (12). In this study, we further examine the effects of the human MPO −463G and −463A transgenes on serum lipids and lesion morphology in LDLR$^{-/-}$ mice. The MPO transgene was correlated with increases in serum cholesterol and triglycerides, weight gain/obesity, and increased lesion size.

METHODS

Animals

Transgenic mice carrying the human −463G and −463A alleles were described previously (12, 23, 24). The mice were generated by microinjection of a 32 kb *Bst*1107I restriction fragment directly into C57BL6/J eggs (12), avoiding the need for backcrossing. To examine the effect of MPO expression in an atherosclerotic model, the mice were crossed to LDLR$^{-/-}$ mice backcrossed for 10 generations onto the C57BL6/J background (Jackson Laboratories). Mice were housed five per cage, maintained at 22°C on a 12 h light/dark cycle, and provided with standard rodent chow or a high-fat atherogenic Western diet (HFD; Harlan Teklad Laboratory; TD 88137) with 42% calories derived from fat (21.2% fat by weight, 0.2% cholesterol) for periods of 9 or 20 weeks. Male and female mice at a mean age of 12.4 weeks (±0.7 SD) were fed a HFD for 9 weeks. Male and female mice at a mean age of 10.2 ± 0.8 weeks were fed a HFD for 20 weeks. The care of the mice, and all procedures used in this study, were approved by our institutional animal care and use committee and complied with National Institutes of Health animal care guidelines.

PCR analysis detected human MPO-flanking sequences in the transgenics, extending at least 7 kb upstream and at least 4–11 kb downstream for the MPOA and MPOG transgenes, respectively. The following PCR primer sets were used: ~7,000 bp upstream (5′-gtatctgaattcagtggaga-3′ and 5′-tttggatttcgctctttcag-3′), ~11 kb downstream (5′-gaatacgtaaagaactctca-3′ and 5′-cctatcagcaatgtatgcat-3′), and ~4 kb downstream (5′-gtgtggaggggagttct-3′ and 5′-ccttggttttcaacagctca-3′). The −463G allele was excised from a sequenced bacterial artificial chromosome clone (accession number AC004687). The −463A allele was from a DNA clone obtained by hybridization screening of a human bacterial artificial chromosome library (Research Genetics) (12).

To determine the sequence of the MPO mRNA produced by the transgenes, we isolated mRNA from bone marrow cells using the Trizol reagent and produced cDNA using oligo(dT) primers and the Omniscript cDNA kit (Qiagen). PCR primers were chosen to amplify in 30 cycles the 2,568 bp cDNA as two ~1,300 bp fragments, and the fragments were subcloned into a plasmid vector for sequencing (Eton Biosciences, San Diego, CA). Sequences obtained were identical to the MPO cDNA sequence reported on GenBank (accession number JO2694). The two transgenic lines are identical at the relatively rare −129G/A polymorphism (A allelic frequency of 0.07) (25), both having the more common −129G residue. Quantitative real-time PCR was used to estimate copy number, using TaqMan MGB probes and primers to compare the threshold cycle for a human MPO intronic sequence with a known mouse single-copy gene, apoB (Applied Biosystems; Sequences on Demand). Results were consistent with single-copy insertions for both the MPOG and MPOA transgenes.

Western blot analysis

Western analysis was carried out on homogenates of bone marrow, brain, kidney, spleen, liver, and heart from control C57BL6/J mice, mouse MPO knockout mice (18), and the MPOG and MPOA transgenics on the mouse MPO knockout background. Cells or tissues were homogenized in SDS sample buffer, and equal amounts of total protein were electrophoresed on 4–20% gradient denaturing SDS-PAGE gels and transferred to polyvinylidene difluoride membranes. Blots were blocked in 5% nonfat dry milk in Tris-buffered saline containing 1% Tween 20 (TBS-T) for 1 h and incubated with polyclonal antibodies to human MPO (BioDesign International) overnight at 4°C in TBS-T with 250 mM NaCl and 5% normal goat serum. Blots were then washed in TBS-T twice at 15 min intervals and incubated with horseradish peroxidase-conjugated secondary antibody for 30 min at room temperature with 5% milk. After two subsequent washes in TBS-T, the blots were developed with ECL reagent (Amersham Biosciences).

Plasma lipid and glucose assays

Mice were fasted overnight, and blood was collected from the retro-orbital sinus under isoflurane anesthesia. Total cholesterol, HDL, triglycerides, and free fatty acid concentrations were determined as described previously (26). HDL-cholesterol was quantitated after precipitation of VLDL and LDL with heparin and manganese chloride. An external control sample with known analyte concentration was run on each plate to ensure accuracy. Plasma glucose concentrations were determined in triplicate using a kit from Sigma.

Atherosclerotic lesion analysis

The heart and proximal aorta were embedded in paraffin, and 5 μm sections were obtained over a 400 μm region spanning

the aortic sinus and valve regions. Every eighth section was collected and stained with Masson's Trichrome. Digital images were obtained and analyzed with Adobe Photoshop®. The lesion areas were outlined extending from the internal elastic lamina (IEL) to the luminal surface and converted to uniform black color, and the number of black pixels was determined using Photoshop®.

Immunohistochemistry

Aortic arch sections were deparaffinized and heat-treated in citrate buffer for antigen retrieval according to standard procedures. Sections were incubated with 10% hydrogen peroxide for 10 min, blocked with 10% goat normal serum for 12 h, incubated overnight with rabbit polyclonal antibody to human MPO (BioDesign International; 1:1,000) or rat monoclonal MOMA2 antibody (Accurate Biochemicals; 1:1,000), followed by biotinylated secondary antibody and avidin-conjugated horseradish peroxidase (Vectastain ABC kit; Vector Laboratories, Burlingame, CA), and detected with peroxidase chromogen kits (DAB nickel, Vector SG, or 3-amino-9-ethylcarbazole; Vector Laboratories). Frozen sections of the aortic arch region were also used for Oil Red O staining and some immunohistochemical analyses. Liver tissue was fixed in 4% paraformaldehyde, and free-floating sections (35 μm) were obtained with a Leica VT1000S vibrating microtome. The sections were stained with antibodies to human MPO (BioDesign International) and monoclonal rat anti-mouse CD68 (Hycult International).

Statistical analysis

Student's *t*-test or ANOVA with Fisher's protected least-squares differences was used to determine statistical significance using Statview software (SAS Institute, Inc., Cary, NC). The data were determined to be appropriate for parametric analysis. All data are presented as means ± SD. $P < 0.05$ was considered significant.

RESULTS

The MPOG and MPOA transgenes produce MPO protein

Analysis of the expression patterns for the MPOG and MPOA transgenics has been reported previously (12). The sequences of the transgenic MPO mRNAs were recently determined and found to be identical to reported sequences (GenBank). PCR analysis revealed at least 7 kb of human MPO upstream sequence in both transgenics and 4–11 kb of downstream sequences in the MPOA and MPOG transgenics. To determine that the human MPO transgenics produce MPO protein, the mice were crossed onto the mouse MPO knockout background (18) to eliminate mouse MPO protein. Western analysis of bone marrow extracts using an antibody generated against human MPO (BioDesign International) did not detect the protein in mouse MPO knockout bone marrow extract but did detect both the heavy (59 kDa) and light (13.5 kDa) chains in MPOG and MPOA transgenic bone marrow cells (**Fig. 1A**), indicating that the MPO precursor protein was correctly processed in the transgenic lines. Western analysis of various tissues showed abundant levels of MPO protein in bone marrow but relatively little to no signal in normal brain, heart, lung, liver, kidney, or spleen (Fig. 1B), consistent with the pattern of MPO expression observed in human tissues.

MPO is present in a subset of aortic lesions in the MPOG- and MPOA-expressing LDLR$^{-/-}$ transgenics

Because macrophages are implicated in atherosclerotic lesions, and the human MPO gene is more inducible in macrophages than is mouse MPO (12), we postulated that the human MPO transgenes would humanize the mouse

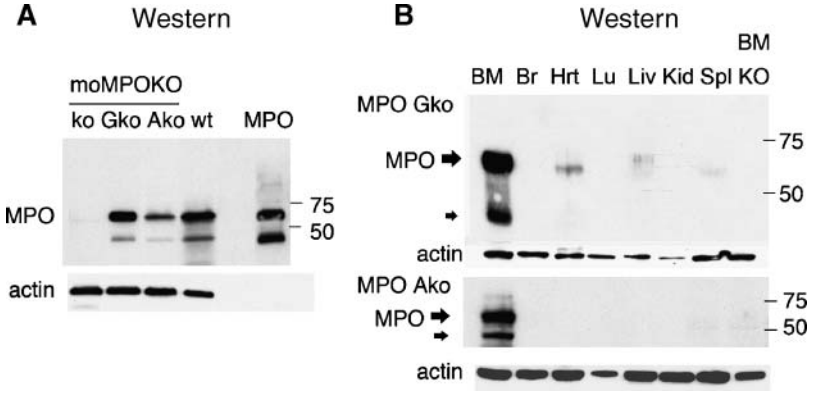

Fig. 1. The myeloperoxidase (MPO) G and A transgenes give rise to MPO protein. A: Western analysis was carried out with bone marrow cell extracts from MPO knockout (ko), MPOG transgenics on the mouse knockout background (Gko), MPOA transgenics on the mouse MPO knockout background (Ako), and wild-type C57BL6/J (wt) and compared with purified human MPO (Calbiochem). Both the MPO heavy and light chains were detected in bone marrow extracts from Gko and Ako using polyclonal antibodies to human MPO (BioDesign International). Protein levels were normalized to mouse β-actin. B: Western analysis of tissue extracts from MPOG or MPOA transgenics on the mouse MPO knockout background. Tissues included bone marrow (BM), brain (Br), heart (Hrt), lung (Lu), liver (Liv), kidney (Kid), spleen (Spl), and, as a control, bone marrow from MPO knockout mice (KO). Arrows indicate MPO protein subunits, with β-actin used for normalization of protein concentration.

atherosclerosis models with regard to MPO. Therefore, we investigated the effects of human MPO transgene expression in the LDLR$^{-/-}$ model. MPO transgenic mice on the LDLR$^{-/-}$ background were fed a HFD for 9 or 20 weeks before analysis of sections throughout the proximal aorta. **Figure 2A** shows an early fatty streak lesion consisting of a cluster of macrophages infiltrating the vascular wall, some with cytoplasmic vesicles characteristic of foam cells. Figure 2B shows a nearby section with strong immunostaining for MPO within the macrophage cluster. Oil Red O staining shows neutral lipid in aortic valve lesions from a female MPOG-expressing LDLR$^{-/-}$ mouse (Fig. 2C) and strong MPO immunostaining in one of three valve lesions in a nearby section (Fig. 2D). These observations indicated that MPO is expressed in cells in a subset of early to intermediate lesions in the MPOG-expressing LDLR$^{-/-}$ model. The finding that MPO was not uniformly expressed in all lesions suggested that the gene is induced in monocyte-macrophages in response to agents at a subset of lesions (12) or that the protein is retained in invading monocytes (5) as a result of such agents. MPO was also detected in lesions in the MPOA-expressing LDLR$^{-/-}$ line (Fig. 2E, F), indicating that MPO is expressed (or retained) in cells at lesions in both transgenic lines. MPO was detected in lesions in both male and female mice; there was no obvious gender difference in the amount of MPO immunodetected in lesions in male or female MPOG- or MPOA-expressing LDLR$^{-/-}$ mice.

MPO was abundant in invading monocyte-macrophages at some advanced lesions, as shown in an example from a male MPOG-expressing LDLR$^{-/-}$ mouse (**Fig. 3**). Masson's Trichrome staining reveals a complex lesion extruded through the IEL into the underlying collagen-rich (blue) adventitia (Fig. 3A). In Fig. 3B, the same section was immunostained for MPO (black) and the macrophage marker MOMA2 (red). MOMA2 staining was detected throughout the lesion, marking the presence of macrophages surrounding angular cholesterol clefts. Aggregations of MPO-positive cells were most apparent at sites where the lesion erupted through the IEL into the adventitia (Fig. 3B, C). MPO-positive cells infiltrating the cap and lesion were more easily seen in an unstained nearby section (Fig. 3D). Costaining for MPO (black) and MOMA2 (red) identified MPO-positive macrophages in

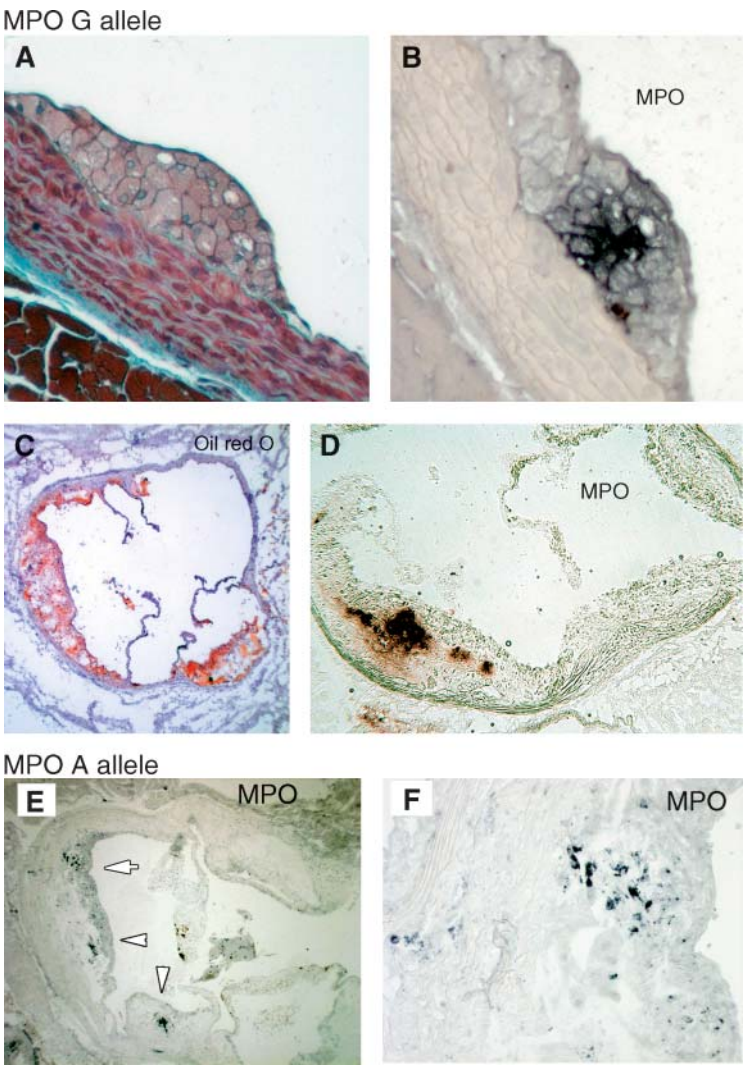

Fig. 2. Atherosclerosis in MPOG- and MPOA-expressing LDL receptor-deficient (LDLR$^{-/-}$) mice fed a high-fat Western diet (HFD). A: Paraffin sections of the aortic root region from a male MPOG-expressing LDLR$^{-/-}$ mouse were stained with Masson's Trichrome stain, showing an aggregation of macrophages in an early fatty streak lesion. B: Polyclonal antibodies to human MPO (BioDesign International) detect abundant MPO in a macrophage cluster in an adjacent section. C: A frozen section from the aortic valve region of a female MPOG-expressing LDLR$^{-/-}$ mouse was stained with Oil Red O to detect neutral lipids. D: An adjacent section shows strong MPO immunostaining in one of three lesions. E: MPO immunostaining was also detected in lesions in a female MPOA-expressing LDLR$^{-/-}$ mouse (arrowheads); a higher magnification image is shown in F. Original objective magnifications are as follows: 20× (A, B, F), 6× (D), and 4× (C, E).

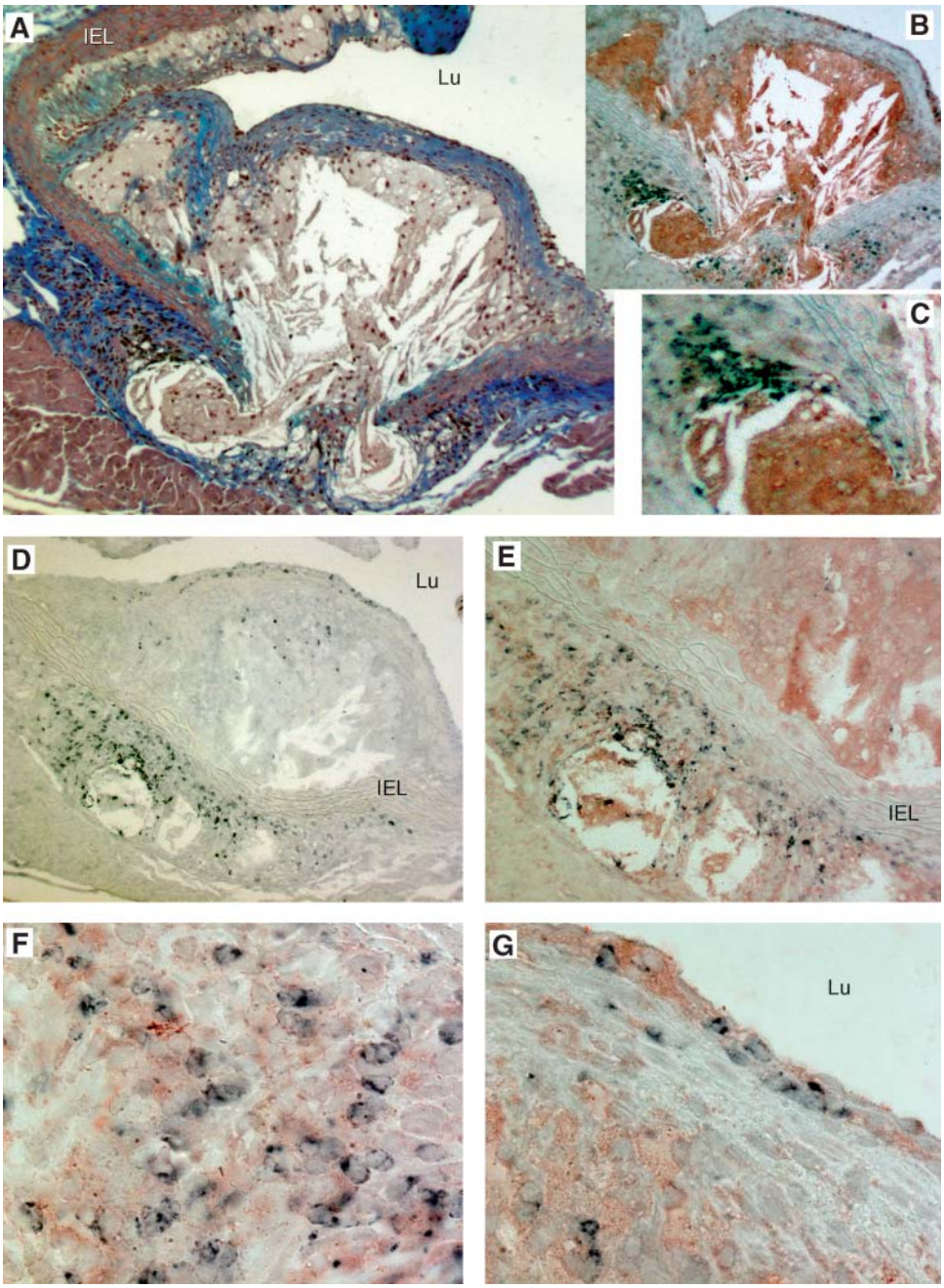

Fig. 3. MPO is detected in macrophages at advanced lesions in MPOG-expressing LDLR$^{-/-}$. Paraffin sections from MPOG-expressing LDLR$^{-/-}$ proximal aorta were stained with Masson's Trichrome (A) after immunostaining for MPO (B–G) and macrophage marker MOMA2 (B, C, E–G). A: Trichrome staining shows a complex lesion erupting through the internal elastic lamina (IEL; red fibers) into the underlying adventitia. Cholesterol clefts appear as clear angular areas. Collagen (blue) staining marks a fibrous cap at the luminal surface. B: The same section was initially stained for MPO (black) and MOMA2 (red). C: Higher magnification shows MPO-positive cells associated with the invading lesion at the point of IEL breakthrough. D: MPO immunostaining of a nearby section shows MPO-positive cells associated with lesions extruded under the IEL and a few MPO-positive cells in the lesion proper and at the luminal surface. E: Higher magnification of the same section costained for MPO (black) and MOMA2 (red) shows colocalization in the area under the IEL. F, G: Higher magnification shows punctate MPO staining in MOMA2-positive macrophages in the sub-IEL area (F) and in macrophages at the luminal cap and infiltrating the lesion (G). Lu, lumen. Original objective magnifications are as follows: 10× (A–D), 20× (E), and 60× (F, G).

the same region beneath the IEL (Fig. 3E). At higher magnification, punctate cytoplasmic MPO staining was seen in macrophages beneath the IEL (Fig. 3F) and in monocyte-macrophages infiltrating from the vessel lumen (Fig. 3G). Consistent with previous reports (18, 19), antibodies to human MPO (BioDesign International) did not detect mouse MPO protein at lesions in the LDLR$^{-/-}$ model (data not shown).

Male MPOG-expressing LDLR$^{-/-}$ transgenics develop higher serum cholesterol and triglycerides

Consistent with earlier findings (27), control LDLR$^{-/-}$ males on the HFD for 20 weeks developed 2-fold higher triglyceride levels than female controls (420 ± 144 vs. 195 ± 88 mg/dl; mean ± SD) (**Fig. 4A**). Similarly, control males on the HFD for 9 weeks developed 1.7-fold higher triglyceride levels than females (216 ± 104 vs. 126 ± 67 mg/dl). The MPOG allele exacerbated this gender difference. Nine week HFD-fed MPOG-expressing LDLR$^{-/-}$ males had 2.3-fold higher triglyceride levels than control LDLR$^{-/-}$ males (502 ± 186 vs. 216 ± 104 mg/dl; $P = 0.0001$). Female MPOG-expressing LDLR$^{-/-}$ mice showed a 1.3-fold increase in triglycerides over control LDLR$^{-/-}$ females, a difference that did not reach statistical significance (163 ± 64 vs. 126 ± 67 mg/dl). Thus, the MPOG allele exacerbated the increase in triglycerides in LDLR$^{-/-}$ males, and there was less effect in females.

In control LDLR$^{-/-}$ mice on the HFD for 9 weeks, cholesterol levels were slightly lower in males than in females (1,340 ± 504 vs. 1,634 ± 205 mg/dl). The MPOG transgene led to a 1.5-fold increase in cholesterol levels in MPOG-expressing LDLR$^{-/-}$ males compared with control LDLR$^{-/-}$ males (2,040 ± 544 vs. 1,340 ± 504 mg/dl; $P = 0.0005$) (Fig. 4B). In contrast, there was no increase in cholesterol levels in MPOG-expressing LDLR$^{-/-}$ females compared with control females (1,669 ± 491 vs. 1,634 ± 205 mg/dl). Unesterified cholesterol was also higher in MPOG-expressing LDLR$^{-/-}$ males than in control males (577 ± 122 vs. 356 ± 132 mg/dl; $P = 0.0005$) (**Table 1**), whereas there was no effect in females attributable to the MPOG transgene (416 ± 111 vs. 410 ± 72 mg/dl). Thus, MPOG increased serum cholesterol in HFD-fed male, but not female, LDLR$^{-/-}$ mice.

Serum glucose levels were higher in MPOG-expressing LDLR$^{-/-}$ males than in control males (281 ± 55 vs. 206 ± 43 mg/dl; $P = 0.002$) (Table 1). Glucose levels increased in female MPOG-expressing LDLR$^{-/-}$ mice compared with female controls, but this trend did not reach significance (231 ± 42 vs. 206 ± 32 mg/dl). Consistent with an earlier report (27), there was no difference in glucose levels between control LDLR$^{-/-}$ males and females on the atherogenic diet (206 ± 43 vs. 206 ± 32 mg/dl).

Consistent results were obtained with mice on the HFD for an extended period of 20 weeks. Cholesterol levels remained significantly higher in MPOG-expressing

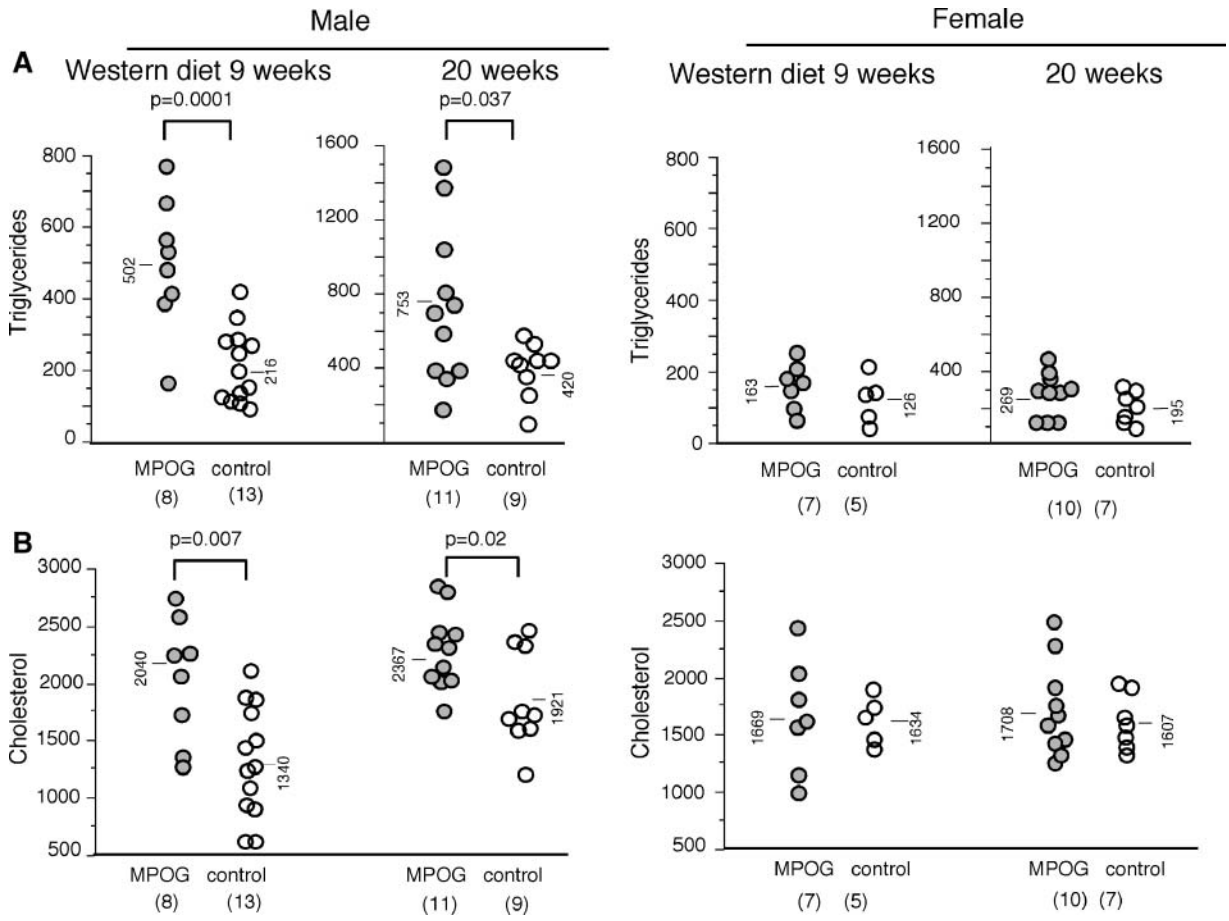

Fig. 4. MPOG-expressing LDLR$^{-/-}$ males have increased cholesterol and triglycerides. Individual serum triglycerides (A) and cholesterol (B) values were determined for a total of 83 male and female MPOG-expressing LDLR$^{-/-}$ and LDLR$^{-/-}$ mice fed the HFD for either 9 or 20 weeks. Mean values are indicated.

TABLE 1. Plasma lipids for MPOG-expressing LDLR$^{-/-}$, control LDLR$^{-/-}$, and MPOA-expressing LDLR$^{-/-}$ male and female mice after 9 weeks or 20 weeks on the high-fat Western diet

	Males			Females		
Variable	MPOG	Control	MPOA	MPOG	Control	MPOA
9 weeks	n = 8	n = 13	n = 9	n = 7	n = 5	n = 4
Total cholesterol	2,040 ± 544 (0.0005)	1,340 ± 504	1,524 ± 303	1,669 ± 491	1,634 ± 205	1,421 ± 146
Unesterified cholesterol	577 ± 122 (0.0005)	356 ± 132	407 ± 63	416 ± 111	410 ± 72	337 ± 39
HDL cholesterol	66 ± 6	71 ± 12	68 ± 11	59 ± 7	58 ± 8	61 ± 7
Triglycerides	502 ± 186 (0.0001)	216 ± 104	227 ± 114	163 ± 64	126 ± 67	120 ± 25
FFAs	80 ± 14	70 ± 12	77 ± 11	69 ± 13	70 ± 19	68 ± 7
Glucose	281 ± 55 (0.002)	206 ± 43	209 ± 21	231 ± 42	206 ± 32	215 ± 32
20 weeks	n = 11	n = 9		n = 10	n = 7	
Total cholesterol	2,367 ± 346 (0.02)	1,921 ± 441		1,708 ± 405	1,607 ± 243	
Unesterified cholesterol	764 ± 109 (0.04)	576 ± 145		509 ± 150	486 ± 82	
HDL cholesterol	106 ± 40	129 ± 33		75 ± 21	83 ± 20	
Triglycerides	753 ± 424 (0.037)	420 ± 144		269 ± 123	195 ± 88	
FFAs	105 ± 21	98 ± 16		78 ± 21	75 ± 19	

LDLR$^{-/-}$, LDL receptor-deficient; MPO, myeloperoxidase. Values shown are mg/dl and are means ± SD. *P* values (in parentheses) refer to differences between MPOG-expressing LDLR$^{-/-}$ and control LDLR$^{-/-}$ mice. *P* values that were not statistically significant are not shown.

LDLR$^{-/-}$ males compared with control males (2,367 ± 346 vs. 1,921 ± 441 mg/dl; $P = 0.02$) (Fig. 4B), although the extended fat diet increased cholesterol levels in the controls, reducing the difference between MPOG-expressing LDLR$^{-/-}$ and control males. Again, the MPOG transgene did not significantly affect cholesterol levels in females (1,708 ± 405 vs. 1,607 ± 243 mg/dl). Triglycerides remained significantly higher in MPOG males compared with control males (753 ± 424 vs. 420 ± 144 mg/dl; $P = 0.037$). Triglycerides were also higher in female MPOG carriers, although this trend did not reach significance (269 ± 123 vs. 195 ± 88 mg/dl; $P = 0.2$). These findings indicate that the MPOG transgene promotes significant increases in serum cholesterol, triglycerides, and glucose in males but has less effect in females.

MPOG-expressing LDLR$^{-/-}$ males gain more weight than LDLR$^{-/-}$ males on the HFD

After 9 weeks on the HFD, the MPOG males gained more weight than control LDLR$^{-/-}$ males (15 vs. 8 g mean weight gain, MPOG-expressing LDLR−/− vs. LDLR−/−; end weight, 40.5 ± 2.7 vs. 33 ± 3.5 g; $P = 0.0001$) (**Fig. 5A**). After 20 weeks on the HFD, the difference remained significant (46.4 ± 3.3 vs. 38.8 ± 5.5 g; $P = 0.0005$). Female MPOG-expressing LDLR$^{-/-}$ and control females gained less weight than males (mean gain of 6.3 vs. 4.8 g, respectively). The MPOG-expressing LDLR$^{-/-}$ females were not significantly heavier than LDLR$^{-/-}$ females at the end of the 9 week period (27.5 ± 3.8 vs. 26.1 ± 2.9 g).

Cholesterol levels were also increased in MPOA-expressing LDLR$^{-/-}$ males (n = 9) (Table 1), although this trend did not reach statistical significance (1,524 ± 303 vs. 1,340 ± 504 mg/dl; $P = 0.23$). However, MPOA males gained more weight than LDLR$^{-/-}$ control males (end weights, 36.1 ± 3.8 vs. 33 ± 3.5 g; $P = 0.04$). As with the MPOG-expressing LDLR$^{-/-}$ females, there was no significant increase in serum lipids (Table 1) or weight in MPOA-expressing LDLR$^{-/-}$ females.

Aortic lesion size

To compare the size of atherosclerotic lesions in the MPOG-expressing LDLR$^{-/-}$ and LDLR$^{-/-}$ mice, serial sections were collected from a 400 μm region spanning the aortic sinus and valve regions. Lesion area was determined with Adobe Photoshop® by outlining the lesions from the IEL to the luminal surface and converting to pixel number as described in Methods. The mean lesion area was significantly larger in MPOG-expressing LDLR$^{-/-}$ compared with LDLR$^{-/-}$ males (182 ± 54 vs. 118 ± 53 × 10^3 μm^2/section; $P = 0.004$) (Fig. 5B). Lesions were also significantly larger in MPOA-expressing LDLR $^{-/-}$ males compared with LDLR$^{-/-}$ males (166 ± 47 × 10^3 μm^2/section; $P = 0.02$). Thus, both MPO transgenes increased the size of lesions in male HFD-fed LDLR$^{-/-}$ mice.

In female HFD-fed LDLR$^{-/-}$ mice, the MPO transgenes did not have a significant effect on lesion size. The mean lesion size was 135 ± 19.6 × 10^3 μm^2/section for MPOG-expressing LDLR$^{-/-}$ females, 120 ± 4 × 10^3 μm^2/section for MPOA-expressing LDLR$^{-/-}$ females ($P = 0.85$), and 124 ± 6.5 × 10^3 μm^2/section for LDLR$^{-/-}$ females (three-way ANOVA; $P = 0.57$ for comparison of MPOG-expressing LDLR$^{-/-}$ with LDLR$^{-/-}$ females, $P = 0.85$ for comparison of MPOA-expressing LDLR$^{-/-}$ with LDLR$^{-/-}$ females, and $P = 0.46$ for comparison of MPOA-expressing LDLR$^{-/-}$ with MPOG-expressing LDLR$^{-/-}$ females).

Regression analysis indicated a correlation between serum cholesterol levels and weight ($R^2 = 0.58$; $P < 0.0001$) for LDLR$^{-/-}$ males, including MPO transgenics and control LDLR$^{-/-}$ males (Fig. 5C). There was also a correlation between cholesterol levels and lesion size ($R^2 = 0.26$; $P = 0.017$) (Fig. 5D). These observations suggest that the increase in serum cholesterol in HFD-fed MPO-expressing LDLR$^{-/-}$ males is related to the increase in weight and lesion size. Photographs of male MPOG-expressing LDLR$^{-/-}$ and LDLR$^{-/-}$ mice illustrate the difference in abdominal size (**Fig. 6A**). There was also a significant correlation between the amount of abdominal fat and body weight in HFD-fed LDLR$^{-/-}$ males in a group including

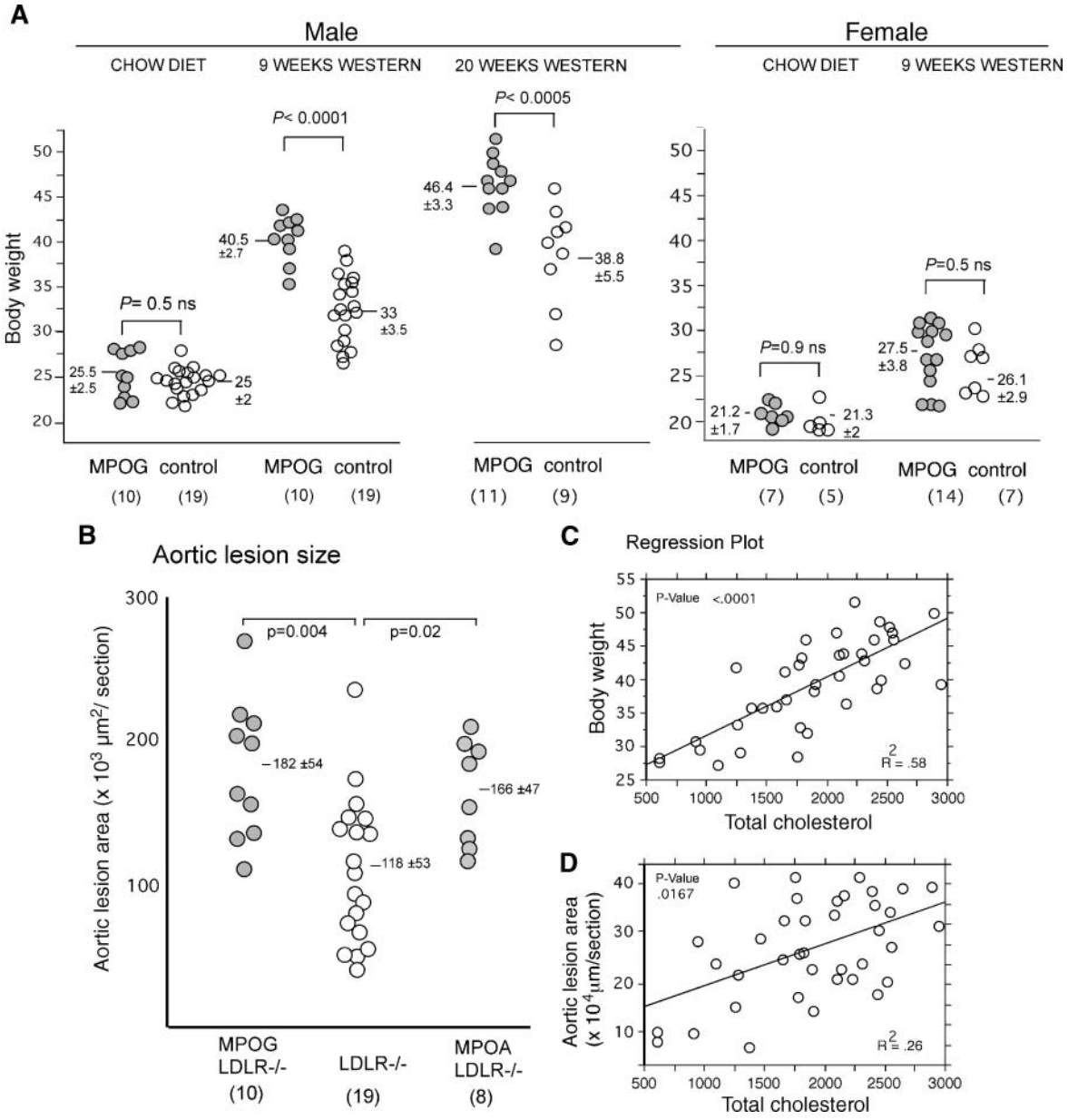

Fig. 5. MPOG-expressing LDLR$^{-/-}$ males exhibit increased body weight correlating with hyperlipidemia and increased size of aortic lesions. A: Individual weights (n = 82) of male and female MPOG-expressing LDLR$^{-/-}$ and LDLR$^{-/-}$ mice fed the normal chow diet or the HFD for 9 or 20 weeks. Means ± SD are shown. B: Mean aortic lesion size ± SD for male MPOG-expressing LDLR$^{-/-}$ (n = 10), LDLR$^{-/-}$ (n = 19), or MPOA-expressing LDLR$^{-/-}$ (n = 8) mice fed the HFD for 9 weeks. C, D: Regression plots show positive correlations between weight and serum cholesterol levels (C) and between lesion size and serum cholesterol levels (D) in LDLR$^{-/-}$ males (including both control LDLR$^{-/-}$ and MPO-expressing LDLR$^{-/-}$ mice). ns, not significant.

MPOG-expressing LDLR$^{-/-}$, MPOA-expressing LDLR$^{-/-}$, and LDLR$^{-/-}$ males (R^2 = 0.701; P = 0.0004) (Fig. 6B).

Human MPO is present in cells lining the hepatic vessels in HFD-fed MPOG-expressing LDLR$^{-/-}$ mice

MPO has been reported to selectively oxidize apolipoproteins, including apoA-I (6, 7), apoB (28), and apoE (29, 30). Such oxidation could influence protein-lipid associations or the uptake of lipoprotein complexes by receptors on hepatocytes or other cells, potentially contributing to the observed increases in serum cholesterol and triglycerides. We examined liver sections of MPOG-expressing LDLR$^{-/-}$ males fed the HFD and detected abundant MPO immunostaining in cells lining hepatic vessels (**Fig. 7C, D**). This intense staining pattern was observed only in HFD-fed MPOG-expressing LDLR$^{-/-}$ males; liver sections from a MPOG male with normal LDLR, fed a normal chow diet, showed relatively few MPO-positive cells surrounding hepatic vessels (Fig. 7A, B). This staining pattern was not observed in HFD-fed MPOA-expressing LDLR$^{-/-}$ liver sections (data not shown). The MPO-positive cells did not colocalize with macrophage marker CD68 (Fig. 7E, F), suggesting that these may not be Kupffer macrophages. Another possible explanation is

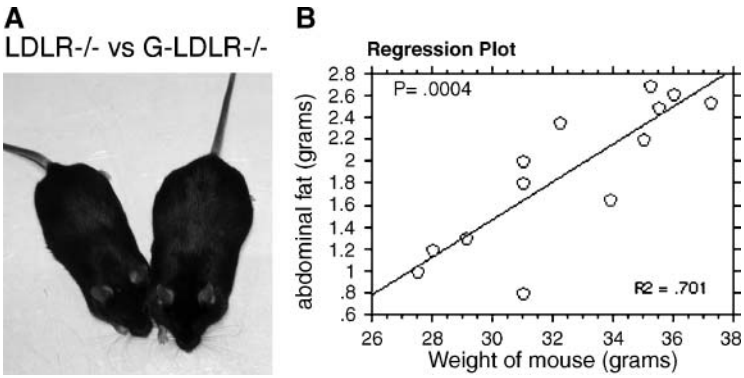

Fig. 6. Correlation between body weight and amount of abdominal fat in male MPOG-expressing LDLR$^{-/-}$ mice. A: LDLR$^{-/-}$ (37 g) and MPOG-expressing LDLR$^{-/-}$ (46 g) males after 20 weeks on the HFD. B: Abdominal fat was weighed and correlated with body weight in MPOG-expressing LDLR$^{-/-}$ and LDLR$^{-/-}$ males on the fat diet for 9 weeks.

that serum MPO may be taken up by hepatocytes or other cells surrounding hepatic vessels.

DISCUSSION

These findings show that the human MPOG and MPOA transgenes are expressed in cells that infiltrate atherosclerotic lesions in LDLR$^{-/-}$ mice fed a HFD. The presence of either the MPOG or MPOA transgene correlated with increased lesion size in males. The higher expressing MPOG allele was linked to hyperlipidemia and weight gain in males but not significantly in females. These observations implicate MPO in atherosclerotic lesion formation and the modulation of serum lipid levels.

Immunohistological examination revealed that MPO was not uniformly present at all lesions but was detected in a subset of early, intermediate, and advanced lesions, suggesting that agents released at particular sites might activate MPO gene expression in monocyte-macrophages (12). Alternatively, agents may preserve MPO protein in infiltrating monocytes (5). A third alternative is that a subset of infiltrating macrophages expresses MPO, resulting in a clonal, nonuniform pattern of expression.

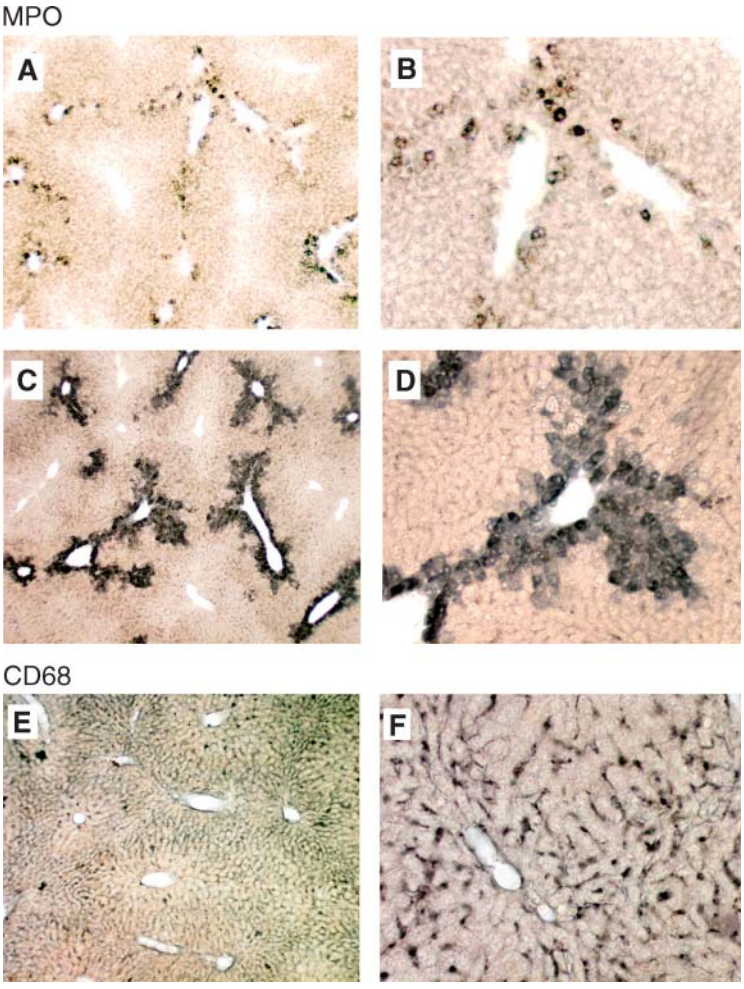

Fig. 7. MPO is abundant in cells lining hepatic vessels in high-fat-fed MPOG-expressing LDLR$^{-/-}$ mice. MPO immunostaining in liver sections is shown for MPOG-expressing LDLR$^{-/-}$ transgenic males on the normal chow diet (A, B) or the HFD (C, D) for 9 weeks. A different pattern of immunostaining was obtained for the macrophage marker CD68 in sections from high-fat-fed MPOG-expressing LDLR$^{-/-}$ mice (E, F). Original objective magnifications are as follows: 4× (A, C, E) and 10× (B, D, F).

MPO-positive macrophages infiltrate the lesions both from the luminal surface and from the underlying adventitia. The latter cells may derive from monocytes that exit small arteries in the adventitia, or they may be tissue macrophages that activate MPO expression in response to inflammatory signals. MPO was most abundant at lesions having cholesterol clefts, suggesting that expression may be induced by oxidized lipids released by necrotic cells. Oxidized LDL (31) or nitrated fatty acids (32) provide ligands for PPARγ, a transcription factor that induces MPO expression (12), especially in the presence of MCSF, which is produced by endothelial cells in response to oxidized LDL (33).

The higher expressing MPOG transgene correlated in males with increases in serum cholesterol, triglycerides, and glucose, along with increased weight gain/obesity. The lower expressing MPOA transgene was also linked to increased body weight, although to a lesser extent than MPOG. This pattern of increased serum glucose, cholesterol, triglycerides, and obesity is suggestive of the metabolic syndrome, associated in humans with increased susceptibility to CAD or peripheral artery disease. These observations suggest that MPO may be involved in modulating serum lipid levels. Earlier studies have suggested that MPO influences reverse cholesterol transport, the process by which excess cholesterol is transferred from peripheral tissues to HDL for delivery to the liver for catabolism and biliary secretion. ABCA1 facilitates cholesterol efflux from foam cell macrophages to lipid-free HDL, reducing or preventing atherosclerosis. MPO selectively oxidizes the apoA-I component of HDL, impairing ABCA1-mediated cholesterol efflux from macrophages (6, 7). MPO also oxidizes apoB (28), a component of LDL, and apoE (29), a component of HDL and VLDL. MPO oxidation of apolipoprotein particles might impair interactions with receptors on hepatic cells, contributing to hyperlipidemia. The finding of high levels of MPO in cells lining hepatic vessels in HFD-fed LDLR$^{-/-}$ mice seems consistent with this possibility. The source of the MPO in cells lining hepatic vessels is unclear, although serum MPO has been found to bind neutrophils through CD11b/CD18 integrins (34) and to bind and transcytose vascular endothelial cells (35). Another possibility is that MPO gene expression may be induced in hepatocytes in hyperlipidemic mice. Although MPO gene expression is generally thought to be myeloid-specific, there are recent reports of the presence of MPO in some reactive nonmyeloid cells, including neurons (36) and astrocytes (37).

Further investigations will be necessary to determine which MPO-expressing cells are most relevant to the observed increases in serum lipids. The MPO present in macrophages at a subset of atherosclerotic lesions may have little effect on serum lipid levels. MPO released by circulating leukocytes may have greater impact as a result of the oxidation of apolipoproteins or receptors, or the MPO present in hepatocytes may affect serum lipids by influencing the uptake or processing of cholesterol.

There was a gender difference in the impact of the MPOG transgene in LDLR$^{-/-}$ mice. Male MPOG-expressing LDLR$^{-/-}$ mice developed higher serum cholesterol, triglycerides, and glucose, correlating with increased body weight/obesity compared with LDLR$^{-/-}$ males, yet the effects in female MPOG-expressing LDLR$^{-/-}$ mice did not reach statistical significance. This gender difference may stem from competition between ER and PPARγ for binding to adjacent sites in the MPO promoter (12). Estrogen blocks the induction of MPO expression by PPARγ ligands, suggesting that estrogen-bound ER enters the nucleus and binds the MPO promoter, blocking binding by PPARγ. The MPO −463A mutation creates a higher affinity ER binding site, correlating with greater estrogen inhibition of PPARγ induction (12). This provides a possible explanation for the reduced impact of the MPOA allele in LDLR$^{-/-}$ mice. In addition, higher estrogen levels in females might explain the reduced impact of the MPOG or MPOA transgene in female LDLR$^{-/-}$ mice. These observations may have relevance to gender differences observed in some human association studies linking the −463G/A polymorphism to risk of chronic inflammatory diseases, including Alzheimer's disease (20, 38, 39), MPO-anti-nuclear cytoplasmic antibody vasculitis (40), and lung cancer (41), and periodontal disease (42).

The MPO transgenes may exacerbate some preexisting gender differences. An earlier study reported that male LDLR$^{-/-}$ mice develop higher triglycerides than female LDLR$^{-/-}$ mice on a high-fat diet (27). The MPOG transgene led to a further increase in triglycerides in male LDLR$^{-/-}$ mice, suggesting that the human MPOG gene exacerbates an existing predilection to hypertriglyceridemia in male LDLR$^{-/-}$ mice. The MPOG transgene also increased serum glucose in male LDLR$^{-/-}$ animals, reminiscent of an earlier report of insulin resistance in male (but not female) LDLR$^{-/-}$ mice (27), again suggesting that MPOG exacerbates an existing predilection in males toward high serum glucose. Further investigations will be necessary to determine whether the −463G/A polymorphism is associated with increased serum lipids in humans, as reported in one study (43), and to reveal the mechanisms underlying the effect of MPO on serum lipids.

Association studies have linked the −463G/A polymorphism to the risk of atherosclerosis/CAD. The higher expressing MPOG allele has been associated with an increased incidence of cardiovascular disease (14, 15), increased frequency of CAD events (13), more rapid progression of atherosclerosis, and reduced coronary flow reserve (16), an indicator of endothelial dysfunction. In other studies, the MPOA allele has been linked to a less favorable outcome after brain infarctions (38), larger fibrotic and calcified aortic lesions (17), and higher serum lipids (43). These findings suggest that MPO may have a dual impact, either positive or negative, or that MPOA may be higher expressing than the MPOG allele in some circumstances, as we reported previously for human peripheral blood mononuclear cells or transgenic macrophages treated with granulocyte-macrophage colony stimulating factor (GMCSF), estrogen, and PPARγ ligands (12).

Prior studies have shown that the MPOG allele is, in most circumstances, higher expressing than the MPOA

allele. The relative expression levels of the MPOG and MPOA alleles, however, can differ dramatically depending on the cell type and the presence of regulatory factors. Quantitative real-time PCR has shown that MPOG is several-fold higher expressing than MPOA in transgenic bone marrow cells and 9-fold higher expressing in MCSF-derived macrophages (12, 24). In the presence of the PPARγ ligand rosiglitazone, MPOG was 294-fold higher expressing than MPOA in MCSF-derived macrophages (12). In human monocyte-derived macrophages, the GG genotype expressed 5- to 7-fold higher MPO mRNA levels than the GA/AA genotypes (12, 24). There were also significant differences between expression levels for the MPOG transgene and the mouse MPO gene. These were expressed at comparable levels in bone marrow cells, whereas in macrophages, MPOG was ~17-fold higher expressing than mouse MPO (12, 24). Thus, the MPOG allele is more susceptible to upregulation in macrophages than MPOA or the mouse MPO gene.

A recent related study found that overexpression of human MPO in the LDLR$^{-/-}$ model led to increased aortic lesion size (19). In that study, bone marrow cells carrying 50 copies of a human MPO cDNA driven by the Visna virus promoter were transplanted into lethally irradiated female LDLR$^{-/-}$ mice. Human MPO was detected in lesions in HFD-fed mice and was associated with larger lesions, but no changes in cholesterol levels or weight were detected. This finding is consistent with our observations that human MPO transgene expression did not lead to increased cholesterol or weight in female LDLR$^{-/-}$ mice. Further comparisons between these two studies are difficult because of possible differences in regulated expression by the human MPO promoter elements versus the Visna virus promoter. The MPOG and MPOA transgenics are driven by extensive (4–11 kb) human MPO-flanking sequences, and the expression pattern is like that seen in human cells, with highest expression in bone marrow precursors. The hyperlipidemia and weight gain observed in this study thus appears to be specially correlated with human MPO transgene expression and not seen with mouse MPO or with the Visna virus promoter-driven cDNA. The human-type MPO expression pattern may be attributable to the Alu-encoded PPARγ binding site, which is not present in mouse MPO or the Visna virus promoter. Both the Visna virus-driven transgenic model and the MPOG and MPOA transgenic models support the role of MPO in atherosclerosis, and both approaches should provide mechanistic insight in future studies.

There appears to be a single copy of either transgene in the MPOG or MPOA transgenic mouse, reducing the likelihood that the observed effects are the result of random insertional events. In addition, the MPOG and MPOA transgenics both led to significant increases in lesion size and body weight in HFD-fed LDLR$^{-/-}$ mice, further arguing against these effects arising from random insertional events that might affect genes other than MPO.

In summary, the main findings of this study are that the human MPO transgenes are appropriately expressed in macrophages at atherosclerotic lesions in HFD-fed LDLR$^{-/-}$ mice and that expression correlates with increased lesion size. The higher expressing MPOG transgene is associated with hyperlipidemia and weight gain in males, with no significant effect in females. Earlier studies suggest a possible explanation for the gender and allelic differences, in that estrogen blocks the strong induction of MPO expression by PPARγ. The PPARγ induction of the MPOA allele, with the stronger ER binding site, is more effectively blocked by estrogen. Mouse models provide an important tool for the analysis of complex multigenic diseases such as atherosclerosis; however, the lack of mouse MPO expression at lesions has impeded studies of MPO involvement. The MPO transgenics should facilitate investigations of the role of MPO in mouse models of atherosclerosis and help decipher the mechanisms underlying the gender-dependent effects on hyperlipidemia and obesity.

This research was supported by grants from the National Institutes of Health: AG-17879 and AG-026539 (to W.F.R.) and HL-30568 (to A.J.L.).

REFERENCES

1. Podrez, E. A., M. Febbraio, N. Sheibani, D. Schmitt, R. L. Silverstein, D. P. Hajjar, P. A. Cohen, W. A. Frazier, H. F. Hoff, and S. L. Hazen. 2000. Macrophage scavenger receptor CD36 is the major receptor for LDL modified by monocyte-generated reactive nitrogen species. *J. Clin. Invest.* **105:** 1095–1108.
2. Eiserich, J. P., M. Hristova, C. E. Cross, A. D. Jones, B. A. Freeman, B. Halliwell, and A. van der Vliet. 1998. Formation of nitric oxide-derived inflammatory oxidants by myeloperoxidase in neutrophils. *Nature.* **391:** 393–397.
3. Daugherty, A., J. L. Dunn, D. L. Rateri, and J. W. Heinecke. 1994. Myeloperoxidase, a catalyst for lipoprotein oxidation, is expressed in human atherosclerotic lesions. *J. Clin. Invest.* **94:** 437–444.
4. Hazen, S. L., J. R. Crowley, D. M. Mueller, and J. W. Heinecke. 1997. Mass spectrometric quantification of 3-chlorotyrosine in human tissues with attomole sensitivity: a sensitive and specific marker for myeloperoxidase-catalyzed chlorination at sites of inflammation. *Free Radic. Biol. Med.* **23:** 909–916.
5. Sugiyama, S., Y. Okada, G. K. Sukhova, R. Virmani, J. W. Heinecke, and P. Libby. 2001. Macrophage myeloperoxidase regulation by granulocyte macrophage colony-stimulating factor in human atherosclerosis and implications in acute coronary syndromes. *Am. J. Pathol.* **158:** 879–891.
6. Bergt, C., S. Pennathur, X. Fu, J. Byun, K. O'Brien, T. O. McDonald, P. Singh, G. M. Anantharamaiah, A. Chait, J. Brunzell, et al. 2004. The myeloperoxidase product hypochlorous acid oxidizes HDL in the human artery wall and impairs ABCA1-dependent cholesterol transport. *Proc. Natl. Acad. Sci. USA.* **101:** 13032–13037.
7. Zheng, L., B. Nukuna, M. L. Brennan, M. Sun, M. Goormastic, M. Settle, D. Schmitt, X. Fu, L. Thomson, P. L. Fox, et al. 2004. Apolipoprotein A-I is a selective target for myeloperoxidase-catalyzed oxidation and functional impairment in subjects with cardiovascular disease. *J. Clin. Invest.* **114:** 529–541.
8. Zhang, R., M. L. Brennan, X. Fu, R. J. Aviles, G. L. Pearce, M. S. Penn, E. J. Topol, D. L. Sprecher, and S. L. Hazen. 2001. Association between myeloperoxidase levels and risk of coronary artery disease. *J. Am. Med. Assoc.* **286:** 2136–2142.
9. Brennan, M. L., M. S. Penn, F. Van Lente, V. Nambi, M. H. Shishehbor, R. J. Aviles, M. Goormastic, M. L. Pepoy, E. S. McErlean, E. J. Topol, et al. 2003. Prognostic value of myeloperoxidase in patients with chest pain. *N. Engl. J. Med.* **349:** 1595–1604.
10. Kutter, D., P. Devaquet, G. Vanderstocken, J. M. Paulus, V. Marchal, and A. Gothot. 2000. Consequences of total and subtotal myeloperoxidase deficiency: risk or benefit? *Acta Haematol.* **104:** 10–15.

11. Piedrafita, F. J., R. B. Molander, G. Vansant, E. A. Orlova, M. Pfahl, and W. F. Reynolds. 1996. An Alu element in the myeloperoxidase promoter contains a composite SP1-thyroid hormone-retinoic acid response element. *J. Biol. Chem.* **271:** 14412–14420.
12. Kumar, A. P., F. J. Piedrafita, and W. F. Reynolds. 2004. Peroxisome proliferator-activated receptor gamma ligands regulate myeloperoxidase expression in macrophages by an estrogen-dependent mechanism involving the −463GA promoter polymorphism. *J. Biol. Chem.* **279:** 8300–8315.
13. Asselbergs, F. W., W. F. Reynolds, J. W. Cohen-Tervaert, G. A. Jessurun, and R. A. Tio. 2004. Myeloperoxidase polymorphism related to cardiovascular events in coronary artery disease. *Am. J. Med.* **116:** 429–430.
14. Nikpoor, B., G. Turecki, C. Fournier, P. Theroux, and G. A. Rouleau. 2001. A functional myeloperoxidase polymorphic variant is associated with coronary artery disease in French-Canadians. *Am. Heart J.* **142:** 336–339.
15. Pecoits-Filho, R., P. Stenvinkel, A. Marchlewska, O. Heimburger, P. Barany, C. M. Hoff, C. J. Holmes, M. Suliman, B. Lindholm, M. Schalling, et al. 2003. A functional variant of the myeloperoxidase gene is associated with cardiovascular disease in end-stage renal disease patients. *Kidney Int. Suppl.* **84:** 172–176.
16. Makela, R., R. Laaksonen, T. Janatuinen, R. Vesalainen, P. Nuutila, O. Jaakkola, J. Knuuti, and T. Lehtimaki. 2004. Myeloperoxidase gene variation and coronary flow reserve in young healthy men. *J. Biomed. Sci.* **11:** 59–64.
17. Makela, R., P. J. Karhunen, T. A. Kunnas, E. Ilveskoski, O. A. Kajander, J. Mikkelsson, M. Perola, A. Penttila, and T. Lehtimaki. 2003. Myeloperoxidase gene variation as a determinant of atherosclerosis progression in the abdominal and thoracic aorta: an autopsy study. *Lab. Invest.* **83:** 919–925.
18. Brennan, M. L., M. M. Anderson, D. M. Shih, X. D. Qu, X. Wang, A. C. Mehta, L. L. Lim, W. Shi, S. L. Hazen, J. S. Jacob, et al. 2001. Increased atherosclerosis in myeloperoxidase-deficient mice. *J. Clin. Invest.* **107:** 419–430.
19. McMillen, T. S., J. W. Heinecke, and R. C. LeBoeuf. 2005. Expression of human myeloperoxidase by macrophages promotes atherosclerosis in mice. *Circulation.* **111:** 2798–2804.
20. Reynolds, W. F., M. Hiltunen, M. Pirskanen, A. Mannermaa, S. Helisalmi, M. Lehtovirta, I. Alafuzoff, and H. Soininen. 2000. MPO and APOEepsilon4 polymorphisms interact to increase risk for AD in Finnish males. *Neurology.* **55:** 1284–1290.
21. Moore, K. J., E. D. Rosen, M. L. Fitzgerald, F. Randow, L. P. Andersson, D. Altshuler, D. S. Milstone, R. M. Mortensen, B. M. Spiegelman, and M. W. Freeman. 2001. The role of PPAR-gamma in macrophage differentiation and cholesterol uptake. *Nat. Med.* **7:** 41–47.
22. Chawla, A., W. A. Boisvert, C. H. Lee, B. A. Laffitte, Y. Barak, S. B. Joseph, D. Liao, L. Nagy, P. A. Edwards, L. K. Curtiss, et al. 2001. A PPAR gamma-LXR-ABCA1 pathway in macrophages is involved in cholesterol efflux and atherogenesis. *Mol. Cell.* **7:** 161–171.
23. Kumar, A. P., C. Ryan, V. Cordy, and W. F. Reynolds. 2005. Inducible nitric oxide synthase expression is inhibited by myeloperoxidase. *Nitric Oxide.* **13:** 42–53.
24. Kumar, A. P., and W. F. Reynolds. 2005. Statins downregulate myeloperoxidase gene expression in macrophages. *Biochem. Biophys. Res. Commun.* **331:** 442–451.
25. Hoy, A., B. Leininger-Muller, O. Poirier, G. Siest, M. Gautier, A. Elbaz, P. Amarenco, and S. Visvikis. 2003. Myeloperoxidase polymorphisms in brain infarction. Association with infarct size and functional outcome. *Atherosclerosis.* **167:** 223–230.
26. Castellani, L. W., P. Gargalovic, M. Febbraio, S. Charugundla, M. L. Jien, and A. J. Lusis. 2004. Mechanisms mediating insulin resistance in transgenic mice overexpressing mouse apolipoprotein A-II. *J. Lipid Res.* **45:** 2377–2387.
27. Li, A. C., K. K. Brown, M. J. Silvestre, T. M. Willson, W. Palinski, and C. K. Glass. 2000. Peroxisome proliferator-activated receptor gamma ligands inhibit development of atherosclerosis in LDL receptor-deficient mice. *J. Clin. Invest.* **106:** 523–531.
28. Carr, A. C., M. R. McCall, and B. Frei. 2000. Oxidation of LDL by myeloperoxidase and reactive nitrogen species: reaction pathways and antioxidant protection. *Arterioscler. Thromb. Vasc. Biol.* **20:** 1716–1723.
29. Jolivalt, C., B. Leininger-Muller, R. Drozdz, J. W. Naskalski, and G. Siest. 1996. Apolipoprotein E is highly susceptible to oxidation by myeloperoxidase, an enzyme present in the brain. *Neurosci. Lett.* **210:** 61–64.
30. Jolivalt, C., B. Leininger-Muller, P. Bertrand, R. Herber, Y. Christen, and G. Siest. 2000. Differential oxidation of apolipoprotein E isoforms and interaction with phospholipids. *Free Radic. Biol. Med.* **28:** 129–140.
31. Nagy, L., P. Tontonoz, J. G. Alvarez, H. Chen, and R. M. Evans. 1998. Oxidized LDL regulates macrophage gene expression through ligand activation of PPARgamma. *Cell.* **93:** 229–240.
32. Baker, P. R., Y. Lin, F. J. Schopfer, S. R. Woodcock, A. L. Groeger, C. Batthyany, S. Sweeney, M. H. Long, K. E. Iles, L. M. Baker, et al. 2005. Fatty acid transduction of nitric oxide signaling: multiple nitrated unsaturated fatty acid derivatives exist in human blood and urine and serve as endogenous peroxisome proliferator-activated receptor ligands. *J. Biol. Chem.* **280:** 42464–42475.
33. Shi, W., M. E. Haberland, M. L. Jien, D. M. Shih, and A. J. Lusis. 2000. Endothelial responses to oxidized lipoproteins determine genetic susceptibility to atherosclerosis in mice. *Circulation.* **102:** 75–81.
34. Lau, D., H. Mollnau, J. P. Eiserich, B. A. Freeman, A. Daiber, U. M. Gehling, J. Brummer, V. Rudolph, T. Munzel, T. Heitzer, et al. 2005. Myeloperoxidase mediates neutrophil activation by association with CD11b/CD18 integrins. *Proc. Natl. Acad. Sci. USA.* **102:** 431–436.
35. Baldus, S., J. P. Eiserich, A. Mani, L. Castro, M. Figueroa, P. Chumley, W. Ma, A. Tousson, C. R. White, D. C. Bullard, et al. 2001. Endothelial transcytosis of myeloperoxidase confers specificity to vascular ECM proteins as targets of tyrosine nitration. *J. Clin. Invest.* **108:** 1759–1770.
36. Green, P. S., A. J. Mendez, J. S. Jacob, J. R. Crowley, W. Growdon, B. T. Hyman, and J. W. Heinecke. 2004. Neuronal expression of myeloperoxidase is increased in Alzheimer's disease. *J. Neurochem.* **90:** 724–733.
37. Choi, D. K., S. Pennathur, C. Perier, K. Tieu, P. Teismann, D. C. Wu, V. Jackson-Lewis, M. Vila, J. P. Vonsattel, J. W. Heinecke, et al. 2005. Ablation of the inflammatory enzyme myeloperoxidase mitigates features of Parkinson's disease in mice. *J. Neurosci.* **25:** 6594–6600.
38. Leininger-Muller, B., A. Hoy, B. Herbeth, M. Pfister, J. M. Serot, M. Stavljenic-Rukavina, L. Massana, P. Passmore, G. Siest, and S. Visvikis. 2003. Myeloperoxidase G−463A polymorphism and Alzheimer's disease in the ApoEurope study. *Neurosci. Lett.* **349:** 95–98.
39. Reynolds, W. F., J. Rhees, D. Maciejewski, T. Paladino, H. Sieburg, R. A. Maki, and E. Masliah. 1999. Myeloperoxidase polymorphism is associated with gender specific risk for Alzheimer's disease. *Exp. Neurol.* **155:** 31–41.
40. Reynolds, W. F., C. A. Stegeman, and J. W. Tervaert. 2002. −463 G/A myeloperoxidase promoter polymorphism is associated with clinical manifestations and the course of disease in MPO-ANCA-associated vasculitis. *Clin. Immunol.* **103:** 154–160.
41. Schabath, M. B., M. R. Spitz, W. K. Hong, G. L. Delclos, W. F. Reynolds, G. B. Gunn, L. W. Whitehead, and X. Wu. 2002. A myeloperoxidase polymorphism associated with reduced risk of lung cancer. *Lung Cancer.* **37:** 35–40.
42. Meisel, P., T. Krause, I. Cascorbi, W. Schroeder, F. Herrmann, U. John, and T. Kocher. 2002. Gender and smoking-related risk reduction of periodontal disease with variant myeloperoxidase alleles. *Genes Immun.* **3:** 102–106.
43. Hoy, A., D. Tregouet, B. Leininger-Muller, O. Poirier, M. Maurice, C. Sass, G. Siest, L. Tiret, and S. Visvikis. 2001. Serum myeloperoxidase concentration in a healthy population: biological variations, familial resemblance and new genetic polymorphisms. *Eur. J. Hum. Genet.* **9:** 780–786.